GLOBAL REGOLITH PROPERTIES FROM DIVINER THERMAL INFRARED MEASUREMENTS. P. O. Hayne[1], J. L. Bandfield[2], A. R. Vasavada[1], R. R. Ghent[3,4], M. A. Siegler[4], J-P. Williams[5], B. T. Greenhagen[6], C. M. Elder[1], D. A. Paige[5] [1]NASA-Jet Propulsion Laboratory, California Institute of Technology (Paul.O.Hayne@jpl.nasa.gov), [2]Space Science Institute, [3]University of Toronto, [4]Planetary Science Institute, [5]University of California, Los Angeles, [6]Applied Physics Laboratory, Johns Hopkins University.

Introduction: The Moon's regolith records the history of fragmentation and overturn by meteorite impacts, which are the dominant geologic processes shaping the lunar surface [1]. Because the impact flux is dominated by the smallest bolides, the upper layers of the lunar surface are overturned and pulverized most frequently [2][3]. Apollo core samples showed depth-dependent density and thermal conductivity profiles, presumably caused by this gradient in overturn timescale [4] and compaction. Local and regional differences in regolith properties may also reveal overturn histories important for understanding cosmic ray exposure ages of individual samples [5].

New Dataset: We used thermal infrared data from the Diviner instrument onboard the Lunar Reconnaissance Orbiter (LRO) to probe the properties of the upper part of the regolith, and map their variations. Diviner is a multi-spectral push-broom imaging radiometer [6], enabling separation of emission from rocks and regolith [7]. Using derived regolith temperatures, we performed least-squares fits to nighttime cooling curves with a numerical heat diffusion model [8][9]. Given the uniformity of the upper regolith structure on the scale of the Diviner measurements [10], we chose to fit the "H-parameter": the vertical *e*-folding scale of the thermal inertia profile.

Results: Global maps of regolith properties were produced from latitude -70 to +70 at a resolution of 128 pixels per degree (~250 m at the equator). Figure 1 shows the resulting map of the H-parameter. Many notable features appear in the H-parameter map, on a range of spatial scales; here we describe only a few of them.

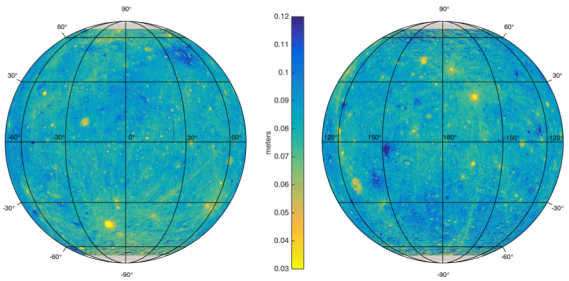

Figure 1: Orthographic maps of the "H-parameter" derived from Diviner nighttime regolith temperatures, scaled to remove latitude dependence. This parameter describes the thermal inertia of the upper ~10-30 cm of regolith, with higher H-values corresponding to lower thermal inertia (higher porosity). The color scale goes from 0.03 to 0.12 m.

Global Scale Patterns: At the largest spatial scales, the most prominent patterns are high thermal inertia materials concentrated in crater rays, and a broad low thermal inertia region correlated with the South Pole Aitken Basin (SPA). We also find a latitude gradient, with lower thermal inertia (higher porosity) at higher latitudes.

Regional Scale Patterns: At scales of ~10 – 100 km, we note the presence of very high thermal inertia regolith within and surrounding large impact craters, as well as the Tycho crater antipode [11]. Low-thermal inertia regolith is found surrounding some fresh impact features, known as "cold spots" [12]. Finally, some low-thermal inertia features on this scale correlate with pyroclastic deposits, though not all pyroclastic deposits exhibit this behavior.

Local Scale Patterns: Regolith properties show distinct variations down to the ~250-m scale of the measurements. Many of these variations are caused by impact processes, and we note an age relationship similar to that identified by [13]. Volcanic features such as irregular mare patches (IMP) also exhibit sometimes strong thermal anomalies, which may be used to constrain their formation mechanisms.

References: [1] McKay, D. S., et al. (1991), *Lunar sourcebook*, 285-356. [2] Gault, D. E., et al. (1974), *LPSC* 5, 2365-2386. [3] Arnold, J. R. (1975), *LPSC* 6, 2375-2395. [4] Carrier W. D. III, Mitchell J. K., and Mahmood A. (1973a), *J. Soil Mech. Found. Div, Am. Soc. Civ. Eng., 99*, 813–832. [5] Langevin, Y., & Arnold, J. R. (1977), *Ann. Rev. Earth and Planet. Sci.*, *5*, 449-489. [6] Paige, D. A., et al. (2010), *Space Sci. Rev.*, *150*(1-4), 125-160. [7] Bandfield, J. L., (2011), *J. Geophys. Res.*, *116*(E12). [8] Hayne, P. O., et al. (2010), *Science*, *330*(6003), 477-479. [9] Hayne, P. O., & Aharonson, O. (2015), *J. Geophys. Res.*, *120*(9), 1567-1584. [10] Vasavada, A. R. et al. (2012), *J. Geophys. Res.*, 117(E12). [11] Bandfield, J. L., et al. (2013), *LPSC,* 44, 1770. [12] Bandfield, J. L., et al. (2014), *Icarus*, *231*, 221-231. [13] Ghent, R. R. et al. (2014) *Geology*, *42*(12), 1059-1062.

Acknowledgements: Part of this work was performed at the Jet Propulsion Laboratory, California Institute of Technology, under contract with the National Aeronautics and Space Administration.